What is the primary function of the early teleost gill? Evidence for Na $^+$/NH$^+_4$ exchange in developing rainbow trout (*Oncorhynchus mykiss*)

Alex M. Zimmer, Patricia A. Wright and Chris M. Wood

Supplementary data	"Data Supplement" http://rspb.royalsocietypublishing.org/content/suppl/2014/09/30/rspb.2014.1422.DC1.html
References	**This article cites 31 articles, 14 of which can be accessed free** http://rspb.royalsocietypublishing.org/content/281/1795/20141422.full.html#ref-list-1
Subject collections	Articles on similar topics can be found in the following collections developmental biology (134 articles) physiology (142 articles)
Email alerting service	Receive free email alerts when new articles cite this article - sign up in the box at the top right-hand corner of the article or click **here**

PROCEEDINGS OF THE ROYAL SOCIETY B

Research

CrossMark
click for updates

Author for correspondence:
Alex M. Zimmer
e-mail: zimmea@mcmaster.ca

Royal Society Publishing

What is the primary function of the early teleost gill? Evidence for Na^+/NH_4^+ exchange in developing rainbow trout (*Oncorhynchus mykiss*)

Alex M. Zimmer[1], Patricia A. Wright[2] and Chris M. Wood[1]

[1]Department of Biology, McMaster University, Hamilton, Ontario, Canada L8S 4K1
[2]Department of Integrative Biology, University of Guelph, Guelph, Ontario, Canada N1G 2W1

Post-hatch fishes lack a functional gill and use cutaneous surfaces for exchange with the surrounding environment. The ionoregulatory hypothesis posits that ionoregulation is the first physiological process to be limited by cutaneous exchange, necessitating its shift to the gills. We hypothesized that the ontogeny of branchial ammonia excretion (J_{amm}) is coupled to Na^+ uptake (J^{Na}_{in}) in accordance with the current model for Na^+/NH_4^+ exchange in freshwater. Using divided chambers, branchial and cutaneous J_{amm}, J^{Na}_{in} and oxygen consumption (MO_2) by larval rainbow trout were assessed. Following hatch, the skin accounted for 97% and 86% of total J_{amm} and J^{Na}_{in}, respectively. J_{amm} and J^{Na}_{in} shifted to the gills simultaneously at 15 days post-hatch (dph) and were highly correlated ($R^2 = 0.951$) at the gills, but not the skin, over development. Contrastingly, MO_2 shifted significantly later at 27 dph, in agreement with the ionoregulatory hypothesis. Moreover, the mRNA expression and/or enzymatic activity of Rhesus proteins, Na^+/H^+-exchanger, H^+-ATPase, Na^+/K^+-ATPase and carbonic anhydrase, all key components of the Na^+/NH_4^+-exchange system, increased in the gills over larval development. We propose that the ontogeny of branchial J^{Na}_{in} occurs as Na^+/NH_4^+ exchange and provide evidence for a novel element to the ionoregulatory hypothesis, the excretion of potentially lethal metabolic ammonia.

1. Introduction

The gill in most teleost fishes is the major site for physiological exchanges with the surrounding environment, participating in gas exchange, ion acquisition, acid-base regulation and nitrogenous waste excretion (reviewed in [1]). In larval fishes, however, the gill is undeveloped following hatch and contributes little to physiological exchange (e.g. [2,3]). Initially, the skin is the dominant site, and as the gills develop, these exchanges eventually shift to become primarily branchial [2,3]. The selective pressures underlying gill ontogeny in both a developmental and evolutionary context have been debated over several decades.

In larval fishes, metabolic rate increases more rapidly over development than skin surface area, leading to a problematic limitation in cutaneous transport, necessitating the development of the gills (reviewed in [4]). August Krogh [5] first suggested that the earliest function of the developing gill is O_2 uptake and this hypothesis, termed the oxygen hypothesis, was the accepted view of gill development for half a century. More recently, however, this view has been challenged. In many fish species, the appearance of branchial ionocytes, the primary site of ionoregulatory exchange, precedes the formation of gill respiratory structures (i.e. filaments or lamellae) [6–8]. These observations led to the ionoregulatory hypothesis, which posits that ionoregulation is the earliest gill function (reviewed in [4,9]). Most recently, Fu *et al.* [3], using divided chambers, directly demonstrated that in rainbow trout larvae reared in soft or hard water, Na^+ uptake shifts from the skin to the gills prior to O_2 uptake, strongly supporting the ionoregulatory hypothesis.

The goal of this study was to determine the relationship between the ontogeny of Na^+ uptake and the ontogeny of excretion of ammonia, the third respiratory gas [10], at this early life stage in an ammoniotelic teleost fish. As recently suggested [9], the ontogeny of branchial ion uptake may occur as a function of homeostatic processes which are coupled to ion uptake such as acid-base balance and/or ammonia excretion, rather than being solely for the acquisition of mineral nutrients. We hypothesized that branchial ammonia excretion in larval trout would occur as a function of Na^+/NH_4^+ exchange and that this coupling of Na^+ uptake (J^{Na}_{in}) and ammonia excretion (J_{amm}) might represent the earliest function of the developing gill. Moreover, J_{amm} in larval fishes is particularly important given that the catabolism of yolk sac proteins, which fuels metabolism at this stage, generates a metabolic ammonia load [11] which can be potentially lethal at elevated levels [12].

In adult rainbow trout, J_{amm} is believed to be coupled to J^{Na}_{in} via an Na^+/NH_4^+-exchange complex in which Rhesus (Rh) glycoproteins play a critical role (reviewed in [13]). However, it is not clear if this would be the case in larval trout where J^{Na}_{in} shifts from the skin to the gills over development [3]. We used the same divided chamber approach as employed by Fu *et al.* [3] to examine these processes. We predicted that, similar to J^{Na}_{in} and oxygen consumption (MO_2) [2,3], J_{amm} would initially occur via cutaneous routes, but would shift to the gills in synchrony with J^{Na}_{in} and not with MO_2. Such a result would indicate that the ontogeny of branchial Na^+ uptake occurs as part of Na^+/NH_4^+-coupled exchange, adding a critical new element to the ionoregulatory hypothesis. Alternatively, if J_{amm} at this stage is not coupled to J^{Na}_{in}, we might expect its shift to be closer to that of another respiratory gas, oxygen. An additional related hypothesis was that J_{amm} and J^{Na}_{in} in larval trout would occur via the components of the Na^+/NH_4^+-exchange complex. We predicted that the increase in branchial J_{amm} and J^{Na}_{in} over development would occur in conjunction with an increase in gene expression and/or enzymatic activity of the key components of the complex (Rh proteins, Na^+/H^+-exchanger (NHE), Na^+/K^+-ATPase, H^+-ATPase and carbonic anhydrase (CA; reviewed in [13]) in the gills, while a decreased mRNA expression and/or activity of these proteins was expected in skin tissues.

2. Material and methods

(a) Fish husbandry

Rainbow trout (*Oncorhynchus mykiss*) embryos were purchased in the eyed-up stage from Rainbow Springs Hatchery (Thamesford, Ontario, Canada) and held at 12°C in hatching trays with flow-through Hamilton dechlorinated tapwater (moderately hard: $[Na^+] = 0.6$ mequiv l^{-1}, $[Cl^-] = 0.8$ mequiv l^{-1}, $[Ca^{2+}] = 0.8$ equiv l^{-1}, $[Mg^{2+}] = 0.3$ mequiv l^{-1}, $[K^+] = 0.05$ mequiv l^{-1}; titration alkalinity 2.1 mequiv l^{-1}; pH approx. 8.0; hardness approx. 140 mg l^{-1} as CaCO3 equivalents). All larvae used in flux experiments and measurements of whole-body ammonia content were from the same batch of embryos which hatched at the same time. Hatching took place approximately one week after purchase and this marked the beginning of the experimental period. Complete yolk sac absorption (CYA) occurred approximately 30 days post-hatch (dph) at which point exogenous feeding began, with daily meals of approximately 5% fish body mass. All experiments performed after CYA were conducted on 48 h fasted fish; experimental temperature was 12°C.

(b) Experimental design for flux measurements

At 0, 3, 6, 9, 12, 15, 18, 21 dph, and following CYA, experiments were conducted to estimate branchial and cutaneous contributions to ammonia excretion (J_{amm}), Na^+ uptake (J^{Na}_{in}) and oxygen consumption (MO_2) using a divided chamber protocol. Prior to experimentation, fish were anaesthetized in 50–100 ppm clove oil, similar to that used in a previous divided chamber study [3]. After anaesthesia to stage 3 [14], each fish was loaded into a small hole in a latex dental dam, such that its head, operculae and pectoral fins were separated spatially from the rest of its body. The fish and dam were then mounted between two 5-ml half-chambers containing dechlorinated tapwater with 10–15 ppm clove oil. Fresh aerated, clove oil-spiked tapwater was then circulated through both chambers using a peristaltic pump at a rate of 0.2 ml min^{-1} for a 1 h acclimation period. An additional control series of experiments was conducted on non-anaesthetized, unrestrained larvae at 3 dph, which revealed that the anaesthetic and divided chamber set-up had no significant effect on J_{amm}, J^{Na}_{in} or MO_2 (data not shown). All experimental procedures, measurements and analyses used for control experiments were identical to those used in the divided chamber experiments described below.

(c) J_{amm} and J^{Na}_{in}

Following the 1 h acclimation period, water recirculation was stopped and 0.5 μCi ^{22}Na (Amersham Pharmacia Biotech Inc.) was added to either the anterior or posterior chamber; it was not possible to measure anterior and posterior Na^+ fluxes on the same fish. Following 5 min of mixing by aeration, initial 1.25 ml samples were taken from both chambers to measure water total ammonia (T_{amm}), Na radioactivity (as counts per minute; cpm) and total $[Na^+]$. Following a 1.5 h flux period, identical final samples were taken, and the remaining water volume was measured in both chambers. Larvae were removed from the divided chambers and were rinsed three times with 5 mM NaCl and once with double-distilled water to remove any surface-bound isotope. Larvae were then euthanized using 0.2 g l^{-1} MS-222, weighed, and counted for ^{22}Na radioactivity. Samples for water T_{amm} were stored at −20°C until later analysis while samples for ^{22}Na radioactivity were counted immediately and stored at 4°C until later $[Na^+]$ analysis. For each flux, a maximum of 10% isotope leak to the unloaded chamber was accepted as a successful dam and all fish recovered completely from anaesthetic treatment within 5 min, prior to euthanasia.

All flux values are presented as flux per gram of whole fish including the yolk sac. Total ammonia concentrations (T_{amm}) of water samples were assayed using the protocol described by Verdouw *et al.* [15]. Anterior and posterior ammonia flux rates (J_{amm}; μmol g^{-1} h^{-1}) were determined using the following equation:

$$J_{amm} = (T_{amm}f - T_{amm}i) \times \frac{V}{t \times M}, \tag{2.1}$$

where $T_{amm}f$ and $T_{amm}i$ are the final and initial concentrations of ammonia (μmol l^{-1}) in the water samples within the anterior or posterior chambers, V is volume (l) of the given chamber, t is flux duration (h) and M is mass (g) of the fish, yolk sac included. Total J_{amm} was determined by adding anterior and posterior flux rates from the same fish. Radioactivity of ^{22}Na in counts per minute (cpm) of water samples and whole larvae was measured via gamma counting (Perkin Elmer Wizard 1480 3″ Auto Gamma Counter), and $[Na^+]$ of water samples was measured using atomic absorption spectrophotometry (SpectrAA 220FS Atomic Absorption Spectrophotometer). Anterior and posterior sodium influx rates (J^{Na}_{in}; μmol g^{-1} h^{-1}) were calculated as

$$J^{Na}_{in} = \frac{R_{fish}}{SA_{average} \times t \times M}, \tag{2.2}$$

where R_{fish} is the gamma-radioactivity of the fish (cpm) at the end of the flux period and $SA_{average}$ is the mean of the initial and final specific activities (cpm/μmol) of the water from the ^{22}Na-loaded chamber. Total J^{Na}_{in} (anterior + posterior) was calculated by sorting replicate fish by mass and pairing corresponding anterior and posterior replicates together.

(d) MO$_2$

O$_2$ consumption rates were measured on separate fish at the same time periods. Following the 1 h acclimation period described above, air lines were removed and anterior and posterior chambers were filled completely with clove oil-spiked tapwater. Initial 600-μl samples were taken from both chambers and replaced with an equal volume of water of known PO$_2$. The PO$_2$ of each initial sample was read immediately using a Clarke-type oxygen electrode (Cameron Instruments) connected to a Model 1900 Polarographic Amplifier (AM Systems) kept at 12°C. Following 0.5–1 h, a second 600 μl sample was taken from each chamber to assess final PO$_2$. This procedure was done simultaneously for both anterior and posterior chambers for each replicate fish. Larvae were then removed from the divided chambers, euthanized and weighed. As in the previous series, 0.5 μCi ^{22}Na was added to one side for the assessment of dam integrity. Anterior and posterior oxygen consumption rates (MO$_2$; μmol g^{-1} h^{-1}) were calculated as

$$MO_2 = \frac{[(PO_2i - PO_2f) \times \alpha O_2 \times V]}{t \times M}, \quad (2.3)$$

where PO$_2i$ (mmHg) is the initial PO$_2$ of the chamber which was corrected for the replacement water of a known PO$_2$ (see above), PO$_2f$ (mmHg) is the final PO$_2$ of the chamber and αO_2 (μmol l^{-1} mmHg^{-1}) is the solubility constant for O$_2$ in water at 12°C [16].

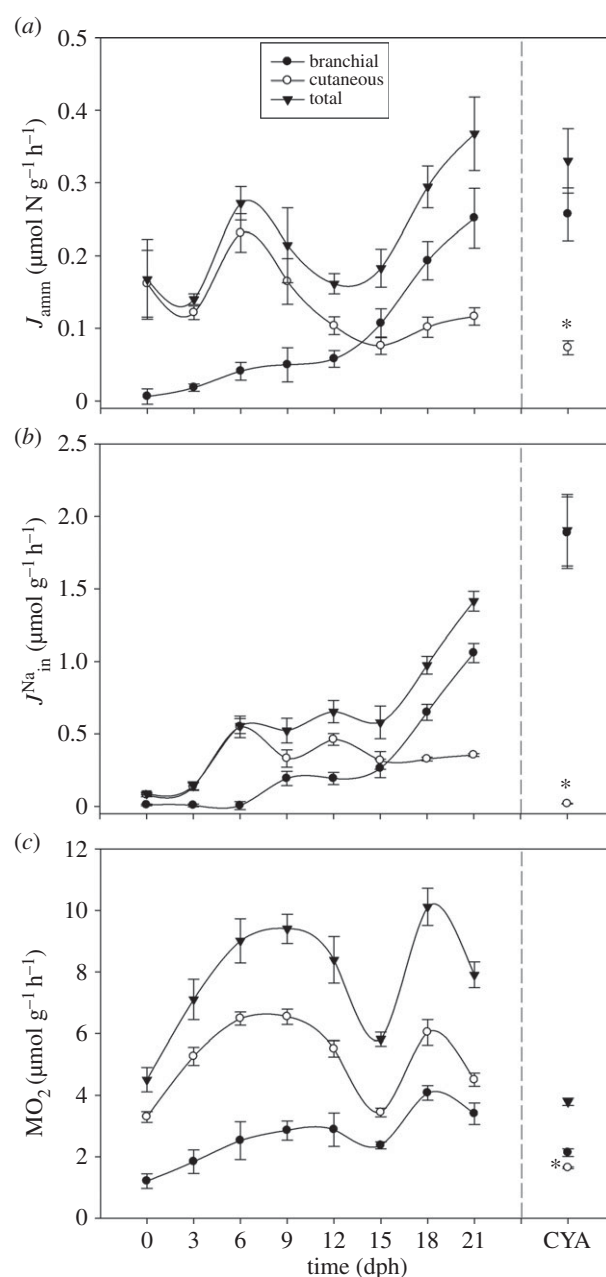## (e) Skin surface area measurements and calculation of branchial and cutaneous flux rates

In a separate batch of larvae, lateral images of larvae at each developmental time point ($n = 3–6$) were taken using a digital camera attached to a Leica EZ4D dissecting microscope. Images were then traced using ImageJ software (Wayne Rasband, National Institutes of Health, USA) and the two-dimensional anterior (head, operculum, pectoral fin) and posterior (body, yolk sac, and dorsal and pelvic fins) surface area (SA) of the lateral aspect of the fish was determined. The resulting proportions of posterior SA relative to total SA over development (% posterior; electronic supplementary material, table S1) were similar to those reported previously using a different method [3]. Branchial flux rates (μmol g^{-1} h^{-1}) were then determined as

$$branchial\ flux\ rate = anterior\ flux\ rate$$
$$- \left[anterior\ SA \times \frac{average\ posterior\ flux\ rate}{posterior\ SA} \right], \quad (2.4)$$

where anterior flux rate (μmol g^{-1} h^{-1}) is the flux measured in the anterior chamber, anterior SA (cm^2) is average anterior cutaneous surface area, average posterior flux rate (μmol g^{-1} h^{-1}) is the average flux measured in the posterior chamber and posterior SA (cm^2) is the average posterior cutaneous surface area. Cutaneous flux rates (μmol g^{-1} h^{-1}) were calculated as

$$cutaneous\ flux\ rate = total\ flux\ rate$$
$$- branchial\ flux\ rate, \quad (2.5)$$

where total flux rate (μmol g^{-1} h^{-1}) is the sum of anterior and posterior flux rates. As in [3], these calculations assume that cutaneous flux per unit skin area is the same in the
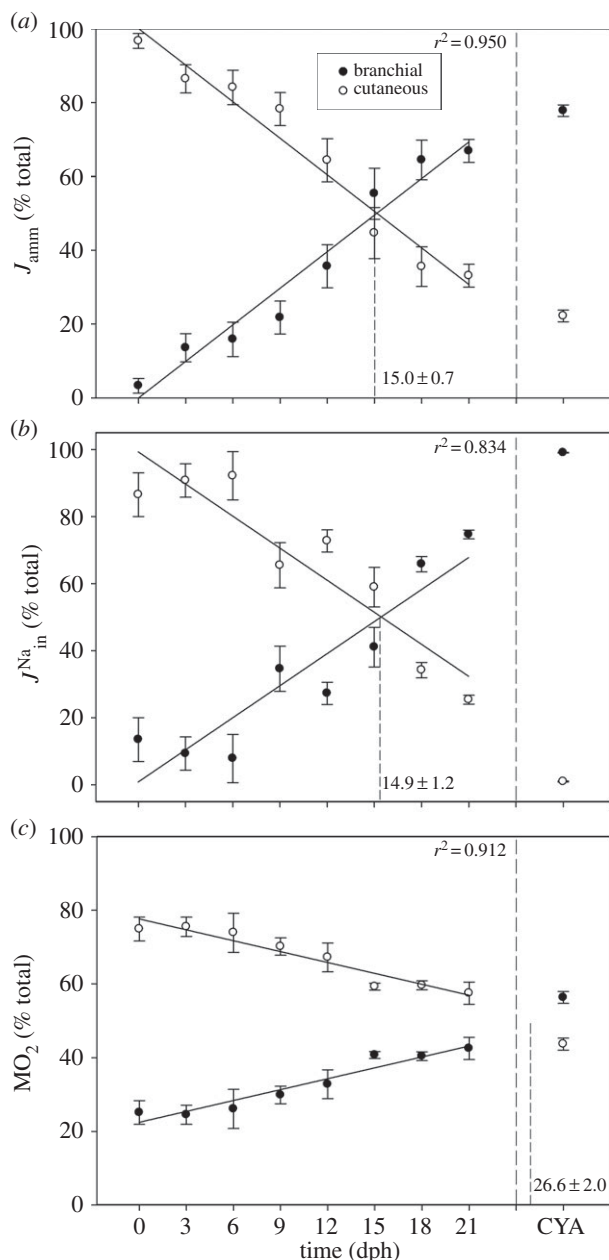
Figure 1. Branchial (filled circles), cutaneous (open circles) and total (filled triangles) of (a) ammonia excretion (J_{amm}), (b) Na$^+$ uptake (J^{Na}_{in}), and (c) oxygen consumption (MO$_2$) rates over development following hatching in rainbow trout. Asterisks represent cutaneous flux rates which differed significantly from corresponding branchial flux rates following CYA. A one-way ANOVA with a multi-comparison Holm–Sidak post hoc test (Dunn's method in the case of failed normality or equal variance tests) revealed that there was a significant difference in J_{amm}, J^{Na}_{in} and MO$_2$ between 0 and 21 days post-hatch. ($n = 6–12$) CYA, complete yolk sac absorption.

head region (i.e. anterior chamber) as in the rest of the body (i.e. posterior chamber).

(f) Estimation of cutaneous-to-branchial shifting point

In order to estimate the cutaneous-to-branchial shifting point for a given process (where 50% occurs via branchial or cutaneous routes), per cent of total branchial and cutaneous values were plotted as x-values against time (dph; y-values). $x = 0$ was then set to 50%, such that the y-intercept (in dph) occurred at $x = 50\%$ and would correspond to the shifting point for any given process. y-intercept values and corresponding standard errors of estimate were obtained using SigmaPlot v. 10.0 (Systat Software, Inc.).
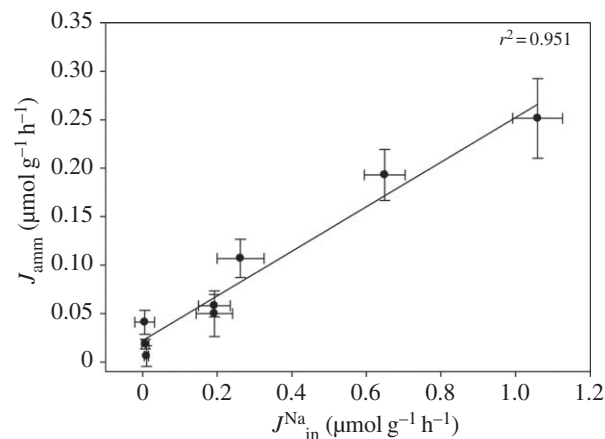
Figure 2. Percentage of branchial (filled circles) and cutaneous (open circles) of (*a*) ammonia excretion (J_{amm}), (*b*) Na$^+$ uptake (J^{Na}_{in}) and (*c*) oxygen consumption (MO$_2$) rates over development following hatching in rainbow trout larvae. Regression analyses were performed using SigmaPlot v. 10.0 with SigmaStat v. 3.5 integration (Systat Software, Inc.). $P \leq 0.0001$ for all regressions. ($n = 6$–12) CYA, complete yolk sac absorption.

Figure 3. The relationship between branchial ammonia excretion (J_{amm}) and Na$^+$ uptake (J^{Na}_{in}) over development following hatching in rainbow trout larvae. Regression analyses were performed using SigmaPlot v. 10.0 with SigmaStat 3.5 integration (Systat Software, Inc.). $r^2 = 0.951$; $p < 0.0001$ ($n = 6$–12).

(h) Branchial and cutaneous enzyme activity and gene expression

At 3, 12, 21 dph, and following CYA, a random set of larvae were removed from hatching trays, euthanized using an overdose of neutralized MS-222; whole gill baskets, yolk sac epithelium and body epithelium samples were taken for gene expression or enzymatic analyses. Tissue samples for gene expression were placed individually directly into 600 µl of ice-cold commercial lysis buffer (PureLink RNA mini kit, Ambion) and homogenized using a small plastic pestle and lysed by passing the homogenate through a 23-gauge needle three times. RNA was extracted from tissue samples using the PureLink RNA mini kit according to the manufacturer's protocol. DNAase treatment was performed using an on-column treatment (PureLink DNAse set, Ambion) also according to the manufacturer's protocol. RNA concentration and purity were determined spectrophotometrically (Nanodrop ND-1000, Nanodrop Technologies) and RNA quality was assessed by running samples through a 1% agarose gel stained with RedSafe (FroggaBio). cDNA was synthesized from 200 ng total RNA using an oligo(dT$_{17}$) primer and superscript II reverse transcriptase (Invitrogen). mRNA expression of reference and target genes was determined by quantitative polymerase chain reaction (qPCR). Total reactions (10 µl) consisted of 4 µl of diluted cDNA template, 5 µl of 2X SsoFast EvaGreen Supermix (Bio-Rad), 0.4 µl each of 100 µmol l^{-1} forward and reverse primers of the genes of interest (electronic supplementary material, table S2), and 0.2 µl nuclease-free water, and were performed using a CFX Connect Real-Time PCR Detection System (Bio-Rad). The reaction mix was first heated to 98°C for 2 min to activate polymerase, followed by 40 amplification cycles of 2 s at 98°C and 5 s at the annealing temperature specific to the given primer pair (electronic supplementary material, table S2) which had been optimized beforehand. No template controls were conducted with every run and non-reverse transcribed controls were performed for every primer pair. Melt curve analyses confirmed the presence of a single PCR product for every gene of interest and the efficiency of amplification for every primer pair in each tissue type was between 95% and 110%. Relative expression of target genes was determined via the ΔΔCq method using both EF1-α and β-actin as reference genes. Expression was normalized to that of the gill at 3 dph using the CFX Manager v. 3.0 software.

For enzymatic analyses, each tissue was placed directly into 250 µl of ice-cold EGTA-Na deoxycholate homogenization buffer, flash frozen and stored at −80°C for later analysis.

(g) Whole-body tissue T_{amm} and turnover time

At 0, 3, 6, 9, 12, 15, 18, 21 dph, and following CYA, a random set of larvae were removed from hatching trays, euthanized in neutralized 0.1 g l^{-1} MS-222, and immediately flash frozen and stored at −80°C. Larvae (1–4 per replicate) were then ground into a fine powder using a liquid N$_2$-cooled mortar and pestle. The powder was deproteinized with 8% HClO$_3$ and subsequently neutralized using 2 M KOH. Whole-body T_{amm} was measured in neutralized, deproteinized samples using a commercial kit (Cliniqa Corporation, San Diego, CA, USA) described in previous studies (e.g. [17]). Ammonia turnover time was calculated as

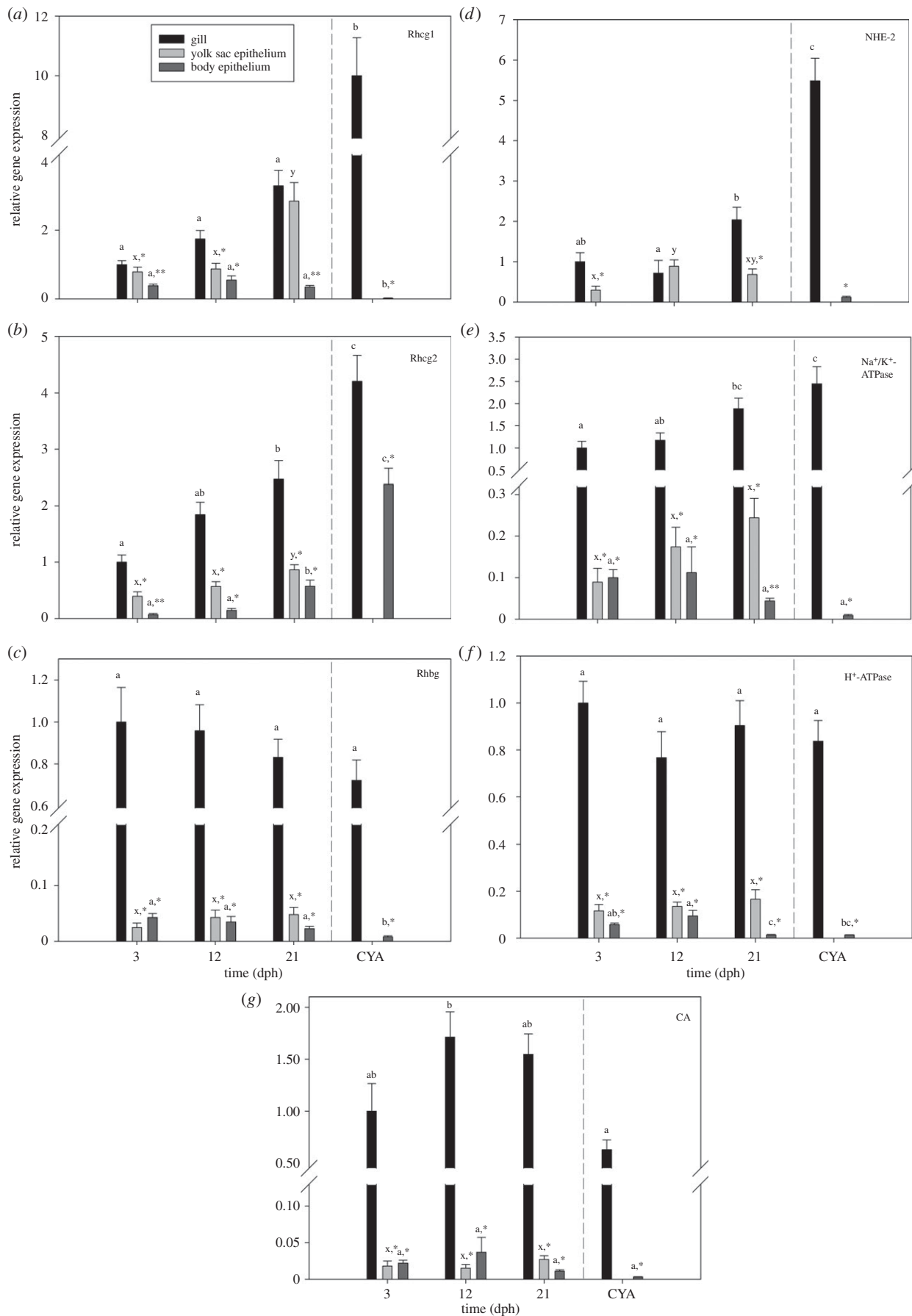$$\text{turnover time} = \frac{\text{whole-body } T_{amm}}{\text{average total } J_{amm}}. \tag{2.6}$$

Figure 4. Relative gene expression of (*a*) Rhcg1, (*b*) Rhcg2, (*c*) Rhbg, (*d*) Na^+/H^+-exchanger-2 (NHE-2), (*e*) Na^+/K^+-ATPase, (*f*) H^+-ATPase and (*g*) CA at 3, 12 and 21 days post-hatch (dph) and after CYA in the gills (black bars), yolk sac epithelium (grey bars) and body epithelium (dark grey bars) of developing rainbow trout larvae. Gene expression is relative to the expression of both EF1-α and β-actin and is normalized to the expression seen in the gill at 3 dph. Means within a given tissue across time points which do not share the same letter are significantly different from one another. Asterisks represent yolk sac epithelium means which differ significantly from gill means within a given time point and double asterisks represent body epithelium means which differ significantly from both gill and yolk sac epithelium means within a given time point. (*n* = 4–6) CYA, complete yolk sac absorption.

Pooling of samples (up to five) was necessary to detect enzyme activity in small tissues. Pooled samples were later homogenized in the EGTA-Na deoxycholate buffer in which they were stored. Na^+/K^+-ATPase, H^+-ATPase and CA activities in homogenates were assayed using methods described previously [18,19]. Protein concentration of homogenates was measured with the Bradford reagent (Sigma) using a bovine serum albumen (Sigma) standard curve.
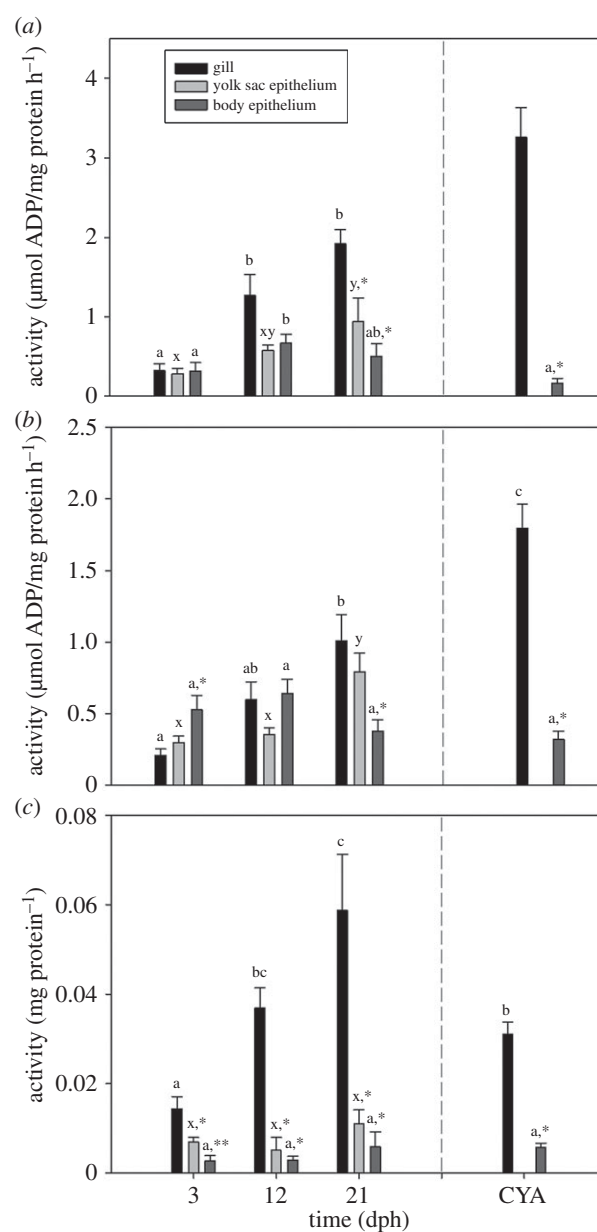
(i) Statistical analyses

All data are represented as means ± 1 s.e.m. (n = sample size) and statistical significance was accepted at the $p < 0.05$ level. All statistical and regression analyses were performed using SigmaPlot v. 10.0 with SigmaStat v. 3.5 integration (Systat Software, Inc.). In general, analyses comparing two means were performed using a two-tailed t-test, whereas analyses comparing three or more means were performed using a one-way analysis of variance (ANOVA) with a Holm−Sidak post hoc test. In the case of a failed normality test, data were square root or log transformed. Specific tests and normalization procedures used are described further in corresponding figure captions.

3. Results and discussion

The ontogeny of J_{amm} and J^{Na}_{in} in larval rainbow trout appears to occur via an Na^+/NH_4^+-exchange complex as seen in the gills of adult trout [13]. Both J_{amm} and J^{Na}_{in} shifted from the skin to the gills at the same time (15 dph) and were highly correlated over development at the gill ($r^2 = 0.951$). Moreover, this shift occurred significantly earlier than that of MO_2 (27 dph), confirming previous work [3] and providing strong support for the ionoregulatory hypothesis. The mRNA expression and/or enzyme activity of several of the key components of the Na^+/NH_4^+-exchange system also increased in the gills, including Rh and NHE, in accordance with the configuration observed in larval zebrafish [20]. The evolution of such exchange systems and metabolons may have occurred as an effective single solution to limitations in a number of cutaneous exchange processes (ions, acid equivalents, nitrogen wastes) over larval development.
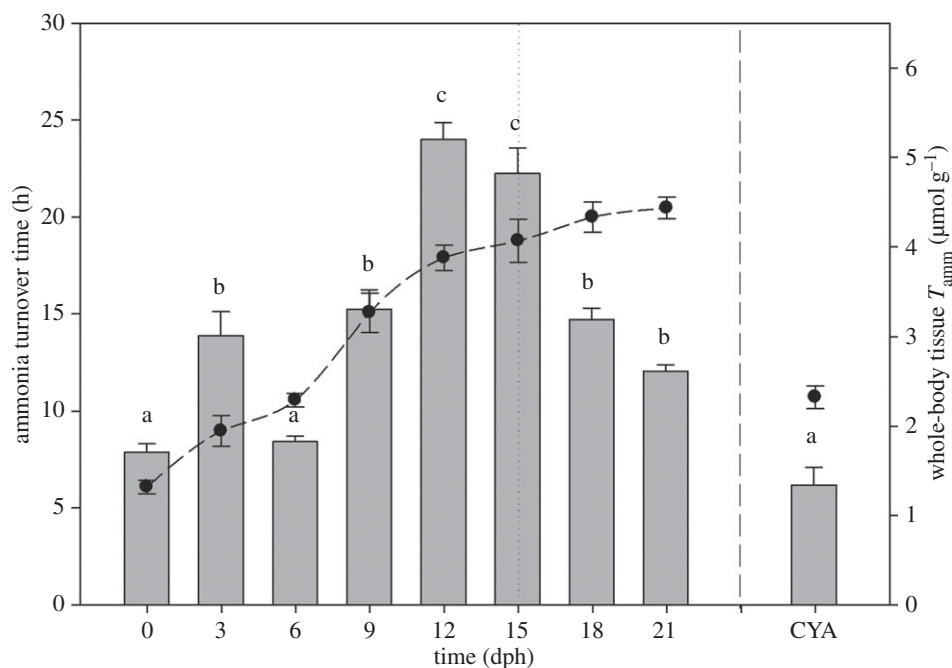
(a) The ontogeny of branchial Na^+/NH_4^+ exchange

Immediately following hatch, the skin represented the dominant site for both J_{amm} and J^{Na}_{in}, accounting for 96.7 ± 2.0 and $86.5 \pm 6.5\%$ of total, respectively (figures 1 and 2). Over development, however, both absolute J_{amm} and absolute J^{Na}_{in} by the gills increased while those by the skin remained relatively constant (figure 1). The cutaneous-to-branchial shift, at which 50% of a given process occurs via the gills, for J_{amm} occurred at 15.0 ± 0.7 dph, remarkably at exactly the same time as J^{Na}_{in} (14.9 ± 1.2 dph), suggesting a coordinated ontogeny of both processes, potentially as Na^+/NH_4^+ exchange. Indeed, both processes were observed to be highly correlated at the gills over development in rainbow trout ($r^2 = 0.951$; figure 3) while, interestingly, such a relationship was not observed at the skin (data not shown). In adult fishes, this coupled exchange is coordinated by a complex consisting of a number of different components (reviewed in [13]). Perhaps the most integral part of the Na^+/NH_4^+-exchange complex is the Rh-NHE metabolon; recent evidence demonstrates that this metabolon is key to both J_{amm} and J^{Na}_{in} in larval fishes [20–23]. In larval rainbow trout, gene expression of Rhcg2 in the gill, relative to 3 dph, increased significantly by

Figure 5. Enzymatic activities of (a) Na^+/K^+-ATPase, (b) H^+-ATPase, (c) CA at 3, 12 and 21 days post-hatch (dph) and after CYA in the gills (black bars), yolk sac epithelium (grey bars) and body epithelium (dark grey bars) of developing rainbow trout larvae. Means within a given tissue across time points which do not share the same letter are significantly different from one another. Asterisks represent yolk sac epithelium means which differ significantly from gill means within a given time point and double asterisks represent body epithelium means which differ significantly from both gill and yolk sac epithelium means within a given time point. ($n = 6-12$) CYA, complete yolk sac absorption.

21 dph, whereas expression of Rhcg1 and NHE-2 increased significantly by CYA (figure 4a,b,d); Rhbg mRNA expression was unchanged in the gills over development (figure 4c). The branchial gene expression of three additional components, Na^+/K^+-ATPase, H^+-ATPase and CA, increased significantly over larval development only in the case of Na^+/K^+-ATPase (figure 4e,f,g). However, the enzymatic activity of these components increased 6.2-, 4.8- and 4.2-fold from 3–21 dph (figure 5) for Na^+/K^+-ATPase, H^+-ATPase and CA, respectively, potentially indicating the induction of at least part of the Na^+/NH_4^+-exchange system. Some discrepancies between gene expression and enzymatic activity may not be surprising

Figure 6. Ammonia turnover times (bars) and whole-body T_{amm} (circles) over development following hatching in rainbow trout larvae. Ammonia turnover time means not sharing the same letter are significantly different from one another as determined by a one-way ANOVA followed by a Holm–Sidak post hoc test following normalization by square root and log transformation, respectively. The dotted line signifies the cutaneous-to-branchial shift for ammonia excretion (15 dph). ($n = 6$) CYA, complete yolk sac absorption.

given that H^+-ATPase, for example, has many regulatory inputs at the post-transcriptional level (reviewed in [24]).

These observations suggest that the ontogeny of branchial Na^+/NH_4^+ exchange is coordinated by the same exchange complex as seen in the gill of adult freshwater fishes [13] and zebrafish larvae [20] and that this arrangement is present at the onset of branchial J_{amm} and J^{Na}_{in}. In the present larval trout, such a configuration does not appear to exist at the skin. Contrary to our initial hypothesis, cutaneous J_{amm} and J^{Na}_{in} (figure 1) and the gene expression and enzyme activity of several of the key components of Na^+/NH_4^+-exchange in cutaneous epithelia (yolk sac and body; figures 4 and 5) remained relatively constant over larval development. This may suggest alternate mechanisms of transport, consistent with differentiation of distinct gill and skin epithelial surfaces. Moreover, the decrease in relative importance of cutaneous routes over development appears to be a function of increasing branchial exchange, rather than decreasing cutaneous exchange.

(b) Evidence supporting a novel element of the ionoregulatory hypothesis

The coordinated cutaneous-to-branchial shifts for J_{amm} and J^{Na}_{in} at 15 dph occurred significantly earlier in development than the shift for MO_2 at 26.6 ± 2.0 dph (by extrapolation, figure 2). These results are in agreement with and nearly identical to those of Fu *et al.* [3], which provided support for the ionoregulatory hypothesis using a direct physiological approach. The independent replication of these results [3] and the wealth of indirect histological evidence that exists (reviewed in [4,9]) provide concrete support for the ionoregulatory hypothesis. Moreover, these findings provide evidence for an additional critical element of the ionoregulatory hypothesis, demonstrating that the ontogeny of branchial Na^+ uptake occurs as Na^+/NH_4^+ exchange.

(c) What is the earliest gill function?

An effective mechanism for excretion of ammonia, the third respiratory gas [10], may be critically important in developing fishes. During larval development, metabolism is fuelled by the catabolism of amino acids obtained from yolk proteins, leading to the release of potentially toxic ammonia. Embryonic fishes, surrounded by the chorion, accumulate a substantial load of metabolic ammonia prior to hatch [25,26]. Whole-body T_{amm} build-up, which continued even after hatch (figure 6), could potentially be attenuated by gill development. Prior to the cutaneous-to-branchial shift for J_{amm}, whole-body T_{amm} accumulated at a rate of 0.18 μmol g d^{-1} over the first 15 dph while from 15 to 21 dph, T_{amm} accumulation slowed to a rate of 0.06 μmol g d^{-1} (figure 6). Similarly, ammonia turnover time increased over development until reaching a peak at 12–15 dph (figure 6), again coinciding with the cutaneous-to-branchial shift for J_{amm} (figure 2). Thereafter, ammonia turnover time decreased steadily, suggesting that the ontogeny of branchial J_{amm} might allow for a more effective clearance of metabolic ammonia. This may be a particularly critical event in early development given the eventual loss of ureogenic capacity which is used in embryonic stages to limit the accumulation of metabolic ammonia [25,27].

The acquisition of mineral ions required by larval growth, however, is also critical to larval development (reviewed in [4]). The simultaneous ontogeny of branchial J_{amm} and J^{Na}_{in} may function to coordinate the elimination of nitrogenous waste, the acquisition of Na^+ and the removal of metabolic acid. At present, it is unclear which of these processes would be the first to be truly limited by cutaneous exchange, necessitating its branchial shift. Gill ablation studies have demonstrated clearly that branchial Na^+ uptake is vital to larval survival earlier in development than branchial O_2 uptake [28] and similar studies may be useful in determining

at which point in development branchial ammonia excretion and acid-base exchange become critical.

(d) Future perspectives

This study, in addition to further affirming and adding a novel element to the ionoregulatory hypothesis, provides evidence that the Na^+/NH_4^+-exchange complex develops at the onset of branchial ontogeny. An interesting avenue for future research is the examination of the selective pressures which led to the evolution of such coupled exchanges. Interestingly, in hagfish, extant relatives of the most ancestral jawless fishes, all of the components of the Na^+/NH_4^+-exchange complex are expressed in the gills [29,30] yet these fish display only Na^+/H^+ exchange and not Na^+/NH_4^+ exchange [31], despite ammonia being the dominant form of nitrogenous waste excreted and the gills accounting for the majority of

its excretion [29,32]. The question of why and when different branchial exchange metabolons evolved in fishes is an interesting one and may lead to a better overall understanding of the arrangement of branchial ionoregulatory, acid-base and nitrogen excretion mechanisms in modern fishes.

References

1. Evans D, Piermarini P, Choe K. 2005 The multifunctional fish gill: dominant site of gas exchange, osmoregulation, acid-base regulation, and excretion of nitrogenous waste. *Physiol. Rev.* **85**, 97–177. (doi:10.1152/physrev.00050.2003)

2. Wells P, Pinder A. 1996 The respiratory development of Atlantic salmon. II. Partitioning of oxygen uptake among gills, yolk sac and body surfaces. *J. Exp. Biol.* **199**, 2737–2744.

3. Fu C, Wilson JM, Rombough PJ, Brauner CJ. 2010 Ions first: Na^+ uptake shifts from the skin to the gills before O_2 uptake in developing rainbow trout, *Oncorhynchus mykiss*. *Proc. R. Soc. B* **277**, 1553–1560. (doi:10.1098/rspb.2009.1545)

4. Rombough PJ. 2007 The functional ontogeny of the teleost gill: which comes first, gas or ion exchange? *Comp. Biochem. Physiol. A. Mol. Integr. Physiol.* **148**, 732–742. (doi:10.1016/j.cbpa.2007.03.007)

5. Krogh A. 1941 *The comparative physiology of respiratory mechanisms*. Philadelphia, PA: University of Pennsylvania Press.

6. Li J, Eygensteyn J, Lock RAC, Verbost PM, Van Der Heijden AJH, Wendelaar Bonga SE, Flik G. 1995 Branchial chloride cells in larvae and juveniles of freshwater tilapia *Oreochromis mossambicus*. *J. Exp. Biol.* **198**, 2177–2184.

7. Gonzalez ME, Blanquez MJ, Rojo C. 1996 Early gill development in the rainbow trout, *Oncorhynchus mykiss*. *J. Morphol.* **229**, 201–217. (doi:10.1002/(SICI)1097-4687(199608)229:2<201::AID-JMOR5>3.0.CO;2-3)

8. Rombough PJ. 1999 The gill of fish larvae. Is it primarily a respiratory or an ionoregulatory structure? *J. Fish Biol.* **55**, 186–204. (doi:10.1111/j.1095-8649.1999.tb01055.x)

9. Brauner CJ, Rombough PJ. 2012 Ontogeny and paleophysiology of the gill: new insights from larval and air-breathing fish. *Respir. Physiol. Neurobiol.* **184**, 293–300. (doi:10.1016/j.resp.2012.07.011)

10. Randall DJ, IP YK. 2006 Ammonia as a respiratory gas in water and air-breathing fishes. *Respir.*

Physiol. Neurobiol. **154**, 216–225. (doi:10.1016/j.resp.2006.04.003)

11. Wright PA, Fyhn JH. 2001 Ontogeny of nitrogen metabolism and excretion. In *Fish physiology*, vol. 20 (eds PA Wright, P Anderson), pp. 149–186. San Diego, CA: Academic Press.

12. Randall DJ, Tsui TKN. 2002 Ammonia toxicity in fish. *Mar. Pollut. Bull.* **45**, 17–23. (doi:10.1016/S0025-326X(02)00227-8)

13. Wright PA, Wood CM. 2009 A new paradigm for ammonia excretion in aquatic animals: role of Rhesus (Rh) glycoproteins. *J. Exp. Biol.* **212**, 2303–2312. (doi:10.1242/jeb.023085)

14. McFarland WN. 1959 A study of the effects of anesthetics on the behaviour and physiology of fishes. *Publ. Inst. Mar. Sci. Univ. Tex.* **6**, 23–55.

15. Verdouw H, van Echteld CJA, Dekkers EMJ. 1978 Ammonia determination based on indophenols formation with sodium salicylate. *Water Res.* **12**, 399–402. (doi:10.1016/0043-1354(78)90107-0)

16. Boutilier RG, Heming TA, Iwama GK. 1984 Physiochemical parameters for use in fish respiratory physiology. In *Fish physiology*, vol. 10 (eds WS Hoar, DJ Randall), pp. 403–430. New York, NY: Academic Press.

17. Zimmer AM, Brauner CJ, Wood CM. 2014 Ammonia transport across the skin of adult rainbow trout (*Oncorhynchus mykiss*) exposed to high environmental ammonia (HEA). *J. Comp. Physiol. B* **184**, 77–90. (doi:10.1007/s00360-013-0784-x)

18. Nawata CM, Hung CCY, Tsui TKN, Wilson JM, Wright PA, Wood CM. 2007 Ammonia excretion in rainbow trout (*Oncorhynchus mykiss*): evidence for Rh glycoprotein and H^+-ATPase involvement. *Physiol. Genomics* **31**, 463–474. (doi:10.1152/physiolgenomics.00061.2007)

19. Zimmer AM, Barcarolli IF, Wood CM, Bianchini A. 2012 Waterborne copper exposure inhibits ammonia excretion and branchial carbonic anhydrase activity in euryhaline guppies acclimated to both fresh

water and sea water. *Aquat. Toxicol.* **122–123**, 172–180. (doi:10.1016/j.aquatox.2012.06.010)

20. Kumai Y, Perry SF. 2011 Ammonia excretion via Rhcg1 facilitates Na^+ uptake in larval zebrafish, *Danio rerio*, in acidic water. *Am. J. Physiol. Regul. Integr. Comp. Physiol.* **301**, R1517–R1528. (doi:10.1152/ajpregu.00282.2011)

21. Shih T-H, Horng J-L, Hwang P-P, Lin L-Y. 2008 Ammonia excretion by the skin of zebrafish (*Danio rerio*) larvae. *Am. J. Physiol. Cell Physiol.* **295**, 1625–1632. (doi:10.1152/ajpcell.00255.2008)

22. Wu S-C, Horng J-L, Liu S-T, Hwang P-P, Wen Z-H, Lin C-S, Lin L-Y. 2010 Ammonium-dependent sodium uptake in mitochondrion-rich cells of medaka (*Oryzias latipes*) larvae. *Am. J. Physiol. Cell Physiol.* **298**, 237–250. (doi:10.1152/ajpcell.00373.2009)

23. Shih T-H, Horng J-L, Liu S-T, Hwang P-P, Lin L-Y. 2012 Rhcg1 and NHE3b are involved in ammonium-dependent sodium uptake by zebrafish larvae acclimated to low-sodium water. *Am. J. Physiol. Regul. Integr. Comp. Physiol.* **302**, R84–R93. (doi:10.1152/ajpregu.00318.2011)

24. Beyenbach KW, Wieczorek H. 2006 The V-type H^+ ATPase: molecular structure and function, physiological roles and regulation. *J. Exp. Biol.* **209**, 577–589. (doi:10.1242/jeb.02014)

25. Wright PA, Felskie A, Anderson P. 1995 Induction of ornithine-urea cycle enzymes and nitrogen metabolism and excretion in rainbow trout (*Oncorhynchus mykiss*) during early life stages. *J. Exp. Biol.* **198**, 127–135.

26. Essex-Fraser PA, Steele SL, Bernier NJ, Murray BW, Stevens ED, Wright PA. 2005 Expression of four glutamine synthetase genes in the early stages of development of rainbow trout (*Oncorhynchus mykiss*) in relationship to nitrogen excretion. *J. Biol. Chem.* **280**, 20 268–20 273. (doi:10.1074/jbc.M412338200)

27. Korte JJ, Salo WL, Cabrera VM, Wright PA, Felski AK, Anderson PM. 1997 Expression of carbamoyl-

phosphate synthetase III mRNA during the early stages of development and in muscle of adult rainbow trout (*Oncorhynchus mykiss*). *J. Biol. Chem.* **272**, 6270–6277. (doi:10.1074/jbc.272.10.6270)

28. Rombough PJ. 2002 Gills are needed for ionoregulation before they are needed for O_2 uptake in developing zebrafish, *Danio rerio. J. Exp. Biol.* **205**, 1787–1794.

29. Braun MH, Perry SF. 2010 Ammonia and urea excretion in the Pacific hagfish *Eptatretus stoutii*: evidence for the involvement of Rh and UT proteins. *Comp. Biochem. Physiol. A* **157**, 405–415. (doi:10.1016/j.cbpa.2010.08.020)

30. Tresguerres M, Parks SK, Goss GG. 2006 V-H$^+$-ATPase, Na$^+$/K$^+$-ATPase and NHE2 immunoreactivity in the gill epithelium of the Pacific hagfish (*Eptatretus stoutii*). *Comp. Biochem.* *Physiol. A* **145**, 312–321. (doi:10.1016/j.cbpa.2006.06.045)

31. Evans DH. 1984 Gill Na$^+$/H$^+$ and Cl$^-$/HCO$_3^-$ exchange systems evolved before the vertebrates entered fresh water. *J. Exp. Biol.* **113**, 465–469.

32. Clifford AM, Guffey SC, Goss GG. 2014 Extrabranchial mechanisms of system pH recovery in hagfish (*Eptatretus stoutii*). *Comp. Biochem. Physiol. A* **168**, 82–89. (doi:10.1016/j.cbpa.2013.11.009)